Article

Projected Changes in Hydrological Extremes in the Yangtze River Basin with an Ensemble of Regional Climate Simulations

Huanghe Gu [1,2,3,*] , **Zhongbo Yu [1,2,3,*]**, **Chuanguo Yang [1,2,3] and Qin Ju [1,2,3]**

[1] State Key Laboratory of Hydrology-Water Resources and Hydraulic Engineering, Hohai University, Nanjing 210098, China; chgyang@gmail.com (C.Y.); super_juqin@126.com (Q.J.)
[2] Joint International Research Laboratory of Global Change and Water Cycle, Hohai University, Nanjing 210098, China
[3] College of Hydrology and Water Resources, Hohai University, Nanjing 210098, China
* Correspondence: ghh0001@hhu.edu.cn (H.G.); zyu@hhu.edu.cn (Z.Y.);
Tel.: +86-13770960371 (H.G.); +86-025-8378-6721 (Z.Y.)

Abstract: This paper estimates the likely impacts of future climate change on streamflow, especially the hydrological extremes over the Yangtze River basin. The future climate was projected by the Coordinated Regional Climate Downscaling Experiment in East Asia (CORDEX-EA) initiative for the periods 2020–2049 under two representative concentration pathways (RCP) 4.5 and 8.5 emission scenarios. The bias corrected outputs from five regional climate models (RCMs) were used in conjunction with the variable infiltration capacity (VIC) macroscale hydrological model to produce hydrological projections. For the future climate of the Yangtze River basin, outputs from an ensemble of RCMs indicate that the annual mean temperature will increase for 2020–2049 by 1.81 °C for RCP4.5 and by 2.26 °C for RCP8.5. The annual mean precipitation is projected to increase by 3.62% under RCP4.5 and 7.65% under RCP8.5. Overall, increases in precipitation are amplified in streamflow, and the change in streamflow also shows significant temporal and spatial variations and large divergence between regional climate models. At the same time, the maximum streamflow in different durations are also projected to increase at three mainstream gauging stations based on flood frequency analysis. In particular, larger increases in maximum 1-day streamflow (+14.24% on average) compared to 5-day and 15-day water volumes (+12.79% and +10.24%) indicate that this projected extreme streamflow increase would be primarily due to intense short-period rainfall events. It is necessary to consider the impacts of climate change in future water resource management.

Keywords: climate change; coordinated regional climate downscaling experiment in East Asia; streamflow; Yangtze River basin

1. Introduction

Global climate observations show an unprecedented warming rate of the atmosphere throughout the last century [1,2]. Rising temperatures are expected to intensify the water cycle due to an increased atmospheric water vapor holding capacity [3,4], leading to the intensification of precipitation extremes as evidenced by both observation and climate model simulations [5–7]. Climate scientists warn that future climate change is unavoidable, these climate warming trends are expected to continue or even amplify [8], and we can expect considerable alterations to atmospheric water vapor concentrations, clouds, precipitation patterns, and runoff and streamflow patterns. Changes in the intensity and distribution of precipitation events under climate change are expected to increase the intensity and frequency of flood events in different parts of the globe [9–14]. Hirabayashi et al. [11] reported that

flooding frequency will increase in 42% and decrease in 18% of the global land area by the end of the 21st century. The combined effects of climate and land-use change in the prairie–pothole region of the United States of America were investigated by Kharel et al. [12], and the results indicated that gradually intensified cropping activities may aggravate the flood threat. Jiang et al. [15] and Chen et al. [16] indicated that eastern China will experience more extreme precipitation events by the end of the 21st century. One important conclusion of these studies is that the projected effects of climate change on flood events may be substantial, but are dependent on the region and climate scenario. The development of adaptation strategies to deal with global warming's potential effects on the hydrologic cycle is still a considerable challenge for water resources management [17].

Because of spatiotemporal differences in climate change and their interactions with society's mitigation, adaptation, and vulnerabilities [18], responses to climate change are highly regionally dependent. This study focuses on the Yangtze River basin in southern China, a region where an increase in precipitation extremes has been observed in the past several decades [19,20]. The Yangtze River basin is home to more than 400 million people and its rich water resources are especially important for several national economies [21]. In addition, the river basin is also home to many endangered species, such as the giant panda, Yangtze River Dolphin, and Yangtze Sturgeon [22]. However, the Yangtze River is also an area where natural disasters happen frequently. In the summer of 1998, flooding of the Yangtze River caused about 3700 deaths, inundated 21.2 million ha of land and caused in excess of US\$30 billion in total direct economic losses [23]. Therefore, planning for climate change's impacts on water resources and flooding in the Yangtze River basin is essential.

The potential impact of climate change on streamflow in the Yangtze River basin has been evaluated in several previous studies at the whole basin or sub-basin scale [24–32]. These studies differ in the selection of global climate models (GCMs), emission scenarios, downscaling method, bias correction method, and hydrological model. There is no doubt that these various factors produce significant differences in the results. The results presented by Xu et al. [29] for seven Coupled Model Intercomparison Project Phase 3 (CMIP3) models with four Special Report on Emissions Scenarios (SRES) indicate increases in mean annual river discharge and flood discharges at the Xiangxi catchment in the Yangtze River basin. The results of the future hydrological projections presented by Su et al. [27], which are based on four hydrological models driven by five bias-corrected CMIP5 GCMs under four representative concentration pathways (RCP) scenarios, project increases in the average and peak discharge in the majority of cases in the 21st century but with significant differences between models. The study of Cao et al. [25] is based on simulations from one regional climate model, RegCM3, linked with a large-scale routing model for scenario SRES A2. However, the results indicate decreases in precipitation and streamflow at the end of the 21st century.

In short, the previous studies assessing the effects of climate change on streamflow in the Yangtze River basin are limited in number, and all the existing studies rely on GCMs or only one regional climate model (RCM) for future climate projections. However, the coarse resolution of GCMs makes it difficult to capture the subgrid-scale physics and fine-scale climate information that are important for a reliable regional impacts assessment [33,34]. A series of studies based on RCMs within the Coordinated Regional Climate Downscaling Experiment in East Asia (CORDEX-EA) has been conducted to project regional climate change and extreme climate vulnerability [35,36]. The higher resolution simulation from the RCMs provides a much better reproduction of the precipitation pattern over the regions with complex terrain, land–sea, and other contrasts. For example, the overestimated precipitation at the eastern edge of the Tibetan Plateau is usually simulated by coarse resolution GCMs, but it is removed by most RCMs [37].

The aim of this study is to project changes in hydrological extremes in the first half of the 21st century in the Yangtze River basin by using multi-model high-resolution regional climate simulations. These future climate projections are obtained from CORDEX-EA simulations under RCP4.5 (medium radiative forcing scenario) and RCP8.5 (high radiative forcing scenario) emission scenarios. Here, RCP4.5 and RCP8.5 are named after the possible radiative forcing (e.g., 4.5 W/m^2 and 8.5 W/m^2,

respectively) expected in the year 2100 relative to pre-industrial values [38]. RCP4.5 assumes global greenhouse gas emissions will peak around 2040, and RCP8.5 assumes that emissions will continue to increase throughout the 21st century. The precipitation and temperature simulated by five RCMs for the periods 1980–2005 and 2020–2049 are used in the hydrological modelling. Such studies have not been undertaken for the Yangtze River basin previously and they provide the first of the high-resolution information necessary to develop climate change adaptation policies related to extreme flood events.

The remainder of the paper is structured as follows: Section 2 describes the study area, observation and climate model data, bias correction, and hydrological modelling methods; the results are presented in Section 3; and the discussion and conclusion are presented in Sections 4 and 5, respectively.

2. Methodology

2.1. Study Area

The Yangtze River is the longest river in China and the third-longest river in the world. It originates from the eastern part of the Tibetan Plateau at an elevation of about 6600 m and runs eastward into the East China Sea near the city of Shanghai (Figure 1). The estimated length of the river is about 6300 km, with a total drainage area of about 1.94×10^6 km^2 [39]. The Yangtze River plays a vital role in Chinese agriculture, industry, and culture. There are various climatic zones and geographical conditions in the Yangtze River basin, from the cold mountain climate in the upper reach to the temperate and sub-tropical climates in the lower reaches. The Yangtze River basin is well known for being prone to flooding because most of the precipitation is brought by the monsoon winds and falls in the summer months [40]. Specifically, the precipitation (primarily falls as snow) at the source region is less than 400 mm/year, whereas the downstream area receives 1600 mm/year. The rainy season from April to October contributes more than 85% of the annual precipitation (~1100 mm/year) [41,42].

Three mainstream stations of the Yangtze River are analyzed in this study: Cuntan (draining 0.87×10^6 km^2), Yichang (draining 1.01×10^6 km^2), and Datong (draining 1.71×10^6 km^2). Cuntan is situated at the upstream limit of the Three Gorges Reservoir, which extends more than 600 km along the mainstream of the Yangtze. The Three Gorges Dam was constructed 37 km upstream of the Yichang hydrological station. Datong is the monitoring station at the lower reach and is located at the tidal limit of the river [42].
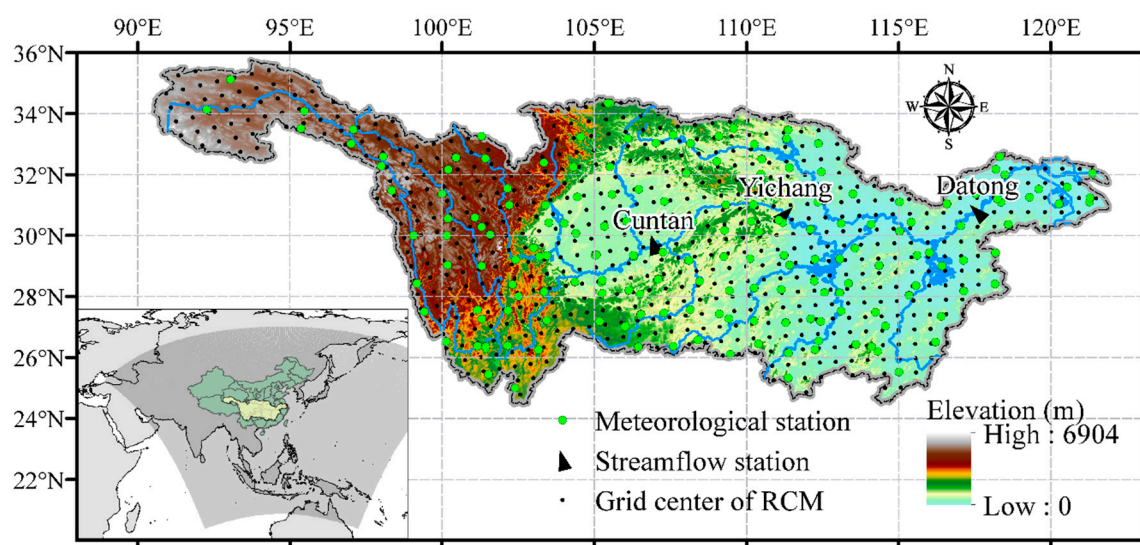

Figure 1. Location of the Yangtze River basin, observation network, and center of the RCM grid cells from the CORDEX simulations. The model domain of the RCMs is shown in the bottom left corner of the figure.

2.2. Watershed Data

Data on daily precipitation and temperature (mean, minimum and maximum) from 178 meteorological stations (159 stations among them have complete data series for the period from 1968 to 2005) used in this study were collected from the China Meteorological Administration. The daily streamflow observations during the period of 1970–2005 at three mainstream hydrological stations (i.e., Cuntan, Yichang, and Datong), which were used to calibrate and validate hydrologic simulations, were collected from the Hydrological Bureau of the Ministry of Water Resources of China. The distribution of the selected meteorological and hydrological gauging stations is shown in Figure 1.

In this study, the Global 30 Arc-Second Elevation (GTOPO30) dataset [43] with 1 km spatial resolution was used for the delineation of the watershed. Soil texture information was obtained based on the Food and Agriculture Organization of the United Nations dataset with about 10 km spatial resolution [44]. The vegetation types were derived from the University of Maryland global land cover classification collected in 1998 with 1 km spatial resolution [45], which had a total of 14 different land cover classes. In this area, grassland and cropland were the two dominant land use types and wooded grassland was the third predominant land use type.

The meteorological observations were gridded to $0.125° \times 0.125°$ grids using the inverse-distance squared method; therefore, the spatial resolution of $0.125° \times 0.125°$ grids is also used in the hydrological model. The resolution of the hydrologic model needs to be high enough to represent the spatial heterogeneity in meteorological, topographical, and soil texture forcing data. The spatial scale at $0.125°$ grid cell for the VIC model used in this study was considered based on the balance between the representation of forcing data and computing time.

2.3. Climate Projection

Five RCMs, which were performed in the framework of the CORDEX experiment for the East Asia domain, were used in this study. As shown in Table 1, these RCMs are HadGEM3-RA, MM5, WRF, RegCM4, and RSM. The whole CORDEX-EA domain includes most of Asia, the Western Pacific, and the South China Sea, as shown in Figure 1. The selected five RCMs have success in modeling and predicting extreme climate as well as in investigating physical processes of East Asian climate [35,46]. More details about the RCMs used in this study can be found in studies from Suh et al. [47] and Park et al. [35]. Each dataset of RCMs consists of historical runs and projections driven by the HadGEM2-AO global climate model under the RCP4.5 and RCP8.5 emission scenarios [38]. The HadGEM2-AO was selected because of its best overall performance in simulating historical annual precipitation in China compared with other the 26 CMIP5 GCMs [48]. The retrieved precipitation and temperature range from 1980 to 2005 for the historical runs and from 2020 to 2050 for the RCPs.

Due to the discrepancy between the RCMs resolution (50 km, except HadGEM3-RA, which is $0.44°$) and the hydrological model ($0.125°$), climate datasets were interpolated to $0.125° \times 0.125°$ grids through the bilinear interpolation method. The interpolated climate data were compared with the original RCM data for the basin, and the differences are small and negligible. For example, in the Yangtze River basin, the annual average precipitation interpolated from HadGEM, MM5, WRF, RegCM, and RSM historical runs (1980–2005) are 1249, 1257, 1326, 1241, and 1581 mm, respectively. The areal precipitation from the original RCMs data are 1241, 1230, 1296, 1218, and 1540 mm respectively (0.6–2.5% differences). Similarly, the differences in annual average temperature between the interpolated climate data and five original RCMs data were less than 0.1 °C.

Table 1. Summary of the five CORDEX East Asia regional climate models used in this study.

RCM	Expansion Name	Institute	Resolution	Reference
HadGEM3-RA	Hadley Centre Global Environmental Model version 3 regional climate model	The Met Office Hadley Centre	$\approx$50 km	[49]
WRF	Fifth-Generation Penn State/NCAR Mesoscale Model	National Center for Atmospheric Research	50 km	[50]
MM5	Fifth-Generation Penn State/NCAR Mesoscale Model	National Center for Atmospheric Research	50 km	[51]
RegCM	Regional Climate Model version 4	The International Centre for Theoretical Physics	50 km	[52]
RSM	Regional Spectral Model	National Centers for Environmental Prediction	50 km	[53]

2.4. Postprocessing of Climate Data: Bias Correction

RCMs are used to dynamically downscale the coarse resolution GCM outputs and explicitly solve mesoscale atmospheric processes for hydrological impact studies. However, they still suffer from considerable biases and therefore are typically adjusted by bias correction methods for hydrological simulations [54]. There are several bias correction methods used in the literature to minimize these errors, ranging from simple adjustments of the mean (in particular, linear scaling) to flexible, potentially multivariate, distribution mapping approaches. Among them, the distribution-based bias correction method is reported to be the best in terms of reproducing the observed climate; it can adjust not only the mean, but also the variance of the RCM precipitation simulation [55]. In this study, we use the bias correction methodology of our previous study in Gu et al. [56]. Specifically, the daily precipitation was corrected by the distribution mapping method, whereas the daily temperature was corrected by the simple linear scaling method because of the relatively moderate deviation of the RCM output.

The distribution transfer between the modelled and observed daily precipitation was completed at each grid. The gamma distribution is often used to represent non-zero precipitation events [57,58]. The cumulative distribution function of gamma distribution is given by

$$cdf(x) = \int_0^x \frac{e^{(-\frac{x}{\theta})}x^{(k-1)}}{\Gamma(k)\theta^k}dx + cdf(0) \tag{1}$$

$$\Gamma(k) = \int_0^{+\infty} t^{k-1}e^{-t}dt \tag{2}$$

where x is the non-zero daily precipitation, $cdf(0)$ is the fraction of days with no precipitation, and k and θ are the shape and rate parameter, respectively.

One of the most common biases of RCM outputs is the overestimation of the wet days with low precipitation. This distorts the precipitation distribution substantially. The RCM-specific wet-day threshold was used to adjust the number of wet days. After that, the modelled and observed daily precipitation were fitted by gamma distribution to determine the parameters with the best fit (k and θ). The transfer function $x_{sim} = f(x_{obs})$ follows the equation $cdf_{sim}(x_{sim}) = cdf_{obs}(x_{obs})$.

Unlike daily precipitation, the modelled daily temperature is expressed in terms of mean, minimum, and maximum temperatures. However, if these three variables are corrected independently by the distribution function transformation, the daily temperature range may result in large errors [59]. The daily temperature was corrected by a sample linear scaling method because of the relatively moderate deviation of the RCM simulation. The correction coefficient for monthly temperature is defined by

$$k_{Tmonth} = \sum_{year=1980}^{2005} \sum_{day=1}^{28,29,30,31} OBS_{year,month,day}(i,j) - \sum_{year=1980}^{2005} \sum_{day=1}^{28,29,30,31} RCM_{year,month,day}(i,j) \tag{3}$$

where *OBS* and *RCM* indicate the observed and modeled daily temperature at a given day (day, month, year), respectively.

2.5. Hydrological Modeling

2.5.1. The VIC Model

Observed and bias-corrected RCM outputs were used as climate forcing for the variable infiltration capacity (VIC) model. The VIC model is a fully distributed and largely physically-based hydrological model originally developed by Xu Liang at the University of Washington [60]. VIC has been successfully used in many regional and global hydrologic studies in a range of climate conditions and resolutions [61–63], including hydrologic simulations of the Yangtze River basin [64,65]. One remarkable character of the model is that it simulates both the water and energy balance near

the land surface such as snow pack accumulation and ablation, canopy interception, surface runoff, evapotranspiration, soil moisture, base flow, and other hydrological processes at daily or sub-daily steps. The land surface was modeled using a mosaic configuration to capture the sub-grid variations in vegetation classes and soil moisture storage capacity [66,67]. Details of the model characteristics can be found in Wood et al. [60], Liang et al. [68], and Li et al. [69]. Because not all climate variables from RCM simulations are available, the minimum set of variables (e.g., daily precipitation, daily max and min temperature, and daily average wind speed) that VIC requires were used in this study. The water balance was the focus of this study, and the surface energy fluxes (sensible heat, ground heat, ground heat storage, outgoing longwave and indirectly latent heat) which also are solved in the VIC model were not evaluated in the present study. The model was run at daily time steps and a $0.125° \times 0.125°$ grid resolution. More than 50,000 dams of various sizes have been built within the Yangtze River basin since 1950 [70]. Due to the large number of dams and the lack of information about their operating procedures, the impacts of these dams are not considered in the hydrological simulation. However, the dams seem to have a limited effect on the streamflow on mainstream hydrological stations because of the large precipitation totals in the wet season [21].

2.5.2. Model Calibration and Validation

The VIC model uses parameters to characterize soil, topography, and vegetation properties. Most of the parameters can be derived from satellite observations or geological surveys, whereas others are typically calibrated to streamflow observations. The model had been previously calibrated for the Yangtze River basin, and these same settings were used in this study [56,71]. Briefly summarized, an automated parameter estimation procedure based on the shuffled complex evolution algorithm was performed in each sub-basin [72], and the percent bias (PBIAS), the coefficient of determination (R^2), and Nash–Sutcliffe coefficient (NSE) [73] between the modeled streamflow and observed value was used to describe the prediction capabilities. The data from 1968 to 2005 were divided into three parts: spin-up (1968–1969), calibration (1970–1979), and validation (1980–2005). The calibrated parameter and their typical ranges are given in Table 2.

Table 2. Calibrated parameter values of the VIC model for the Yangtze River basin.

Parameter	Physical Meaning	Realistic Range	Value
b	Exponent of variable infiltration capacity curve	0–10.0	0.4
D_m	Maximum velocity of baseflow (mm/day)	0–30	10
D_s	Fraction of D_m where non-linear baseflow begins	0–1.0	0.56
W_s	Fraction of maximum soil moisture where non-linear baseflow begins	0–1.0	0.65
d_1	Thickness of the first soil layer (m)	0.05–2.0	0.1
d_2	Thickness of the second soil layer (m)	0.05–2.0	0.3
d_3	Thickness of the third soil layer (m)	0.05–2.0	1.0

Figure 2 shows the results of daily streamflow at three mainstream hydrological stations for the calibration (1970–1979) and validation (1980–2005) periods. The performance of the VIC model confirms that the model could simulate the daily streamflow pattern and magnitude well during the calibration period with the values of PBIAS and NSE varying from -0.8% to -3.2%, and 0.81 to 0.88, respectively. In the validation period, the PBIAS values vary from -1.8% to -2.7%, and the NSE values are lower, ranging from 0.75 to 0.85, but the model could reproduce the streamflow processes reasonably well. According to Moriasi et al. [74], the results for the three hydrological stations can be classified to be 'good' (e.g., $\pm 2.5\% <$ PBIAS $< \pm 15\%$, $0.70 \leq$ NSE ≤ 0.80) or even 'very good' (e.g., PBIAS $< \pm 2.5\%$, NSE > 0.80) for daily streamflow simulation.

The annual maximum 1-day, 5-day, 10-day, and 15-day streamflows simulated by the VIC model were evaluated because the extreme hydrological event was another primary concern in this study. As shown in Figure 2, the coefficient of determination (R^2) of these simulations ranges from 0.73 to

0.92, and the PBIAS in most simulations was less than 10% (except the maximum one-day and five-day streamflow at Datong station).

These parameters in the VIC model are therefore effective for streamflow simulation in the Yangtze River basin. Under the assumption that there are no significant changes in soil and vegetation properties due to future climate change, the model parameters used are unchanged for hydrological simulation in future periods. It should be noted that part of the error in streamflow extremes simulations arises from the low density of the meteorological stations used in this study. Based on this, it is difficult for the model to produce strongly realistic streamflow extremes during historical period.

The dams (mostly in tributaries of the Yangtze River) seem to have little effect on the streamflow at the three mainstream stations because of the excellent match between the model-simulated and measured daily streamflow for the calibration period (1970–1979) and the validation period (1980–2005). On the other hand, the model may have considered some of the human impacts through the model calibration to match the observation. In reality, the hydrological regime is also influenced by various human activities, such as dam construction, water transfer project, agricultural irrigation, and urbanization. A hydrological model that considers all these human activities is being developed. For now, this study mainly focuses on the impact of climate change on hydrological regimes. Therefore, the results of this study are intended to provide overall and regional trends across the whole Yangtze River basin rather than to get a precise prediction at a specific location.
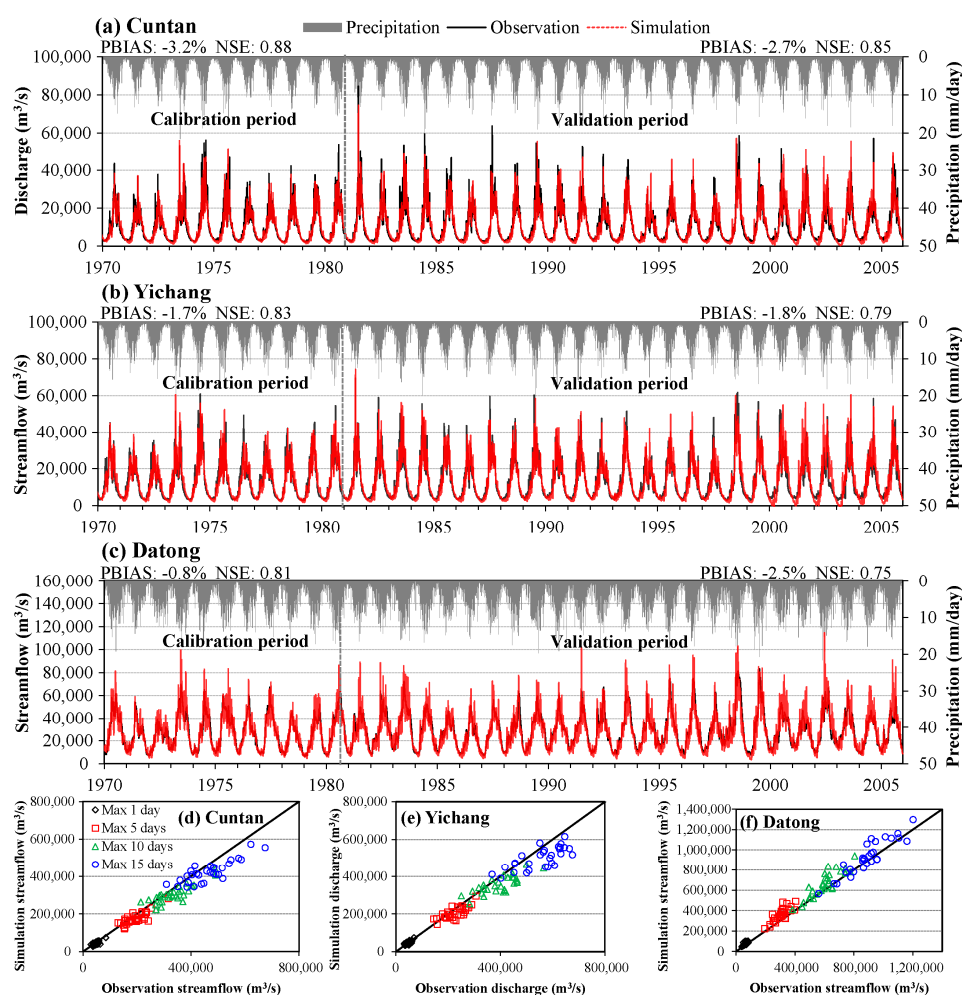

Figure 2. The observed and simulated daily streamflow time series plots and annual maximum 1-day, 5-day, 10-day, and 15-day streamflow scatter plots (bottom panel) in the calibration (1970–1979) and validation (1980–2005) periods at (**a**,**d**) Cuntan, (**b**,**e**) Yichang, and (**c**,**f**) Datong.

2.5.3. Flood Frequency Analysis

The rigorously calibrated and validated VIC model was then used to simulate daily streamflow in each catchment for the historical reference period (1980–2005) and the future scenario period (2020–2049). It should also be noted that two more years of each period were considered as the spin-up period of the VIC model. Floods are random multivariate events and can be described by different variables (such as peak flows, volumes, durations, and shapes). For the design of some hydraulic structures where storage is involved, both peak flow and the entire hydrograph (or at least volume estimates) are required [75]. In this study, the peak flow was represented by the annual maximum 1-day streamflow, and the flood volume and duration were represented by the annual maximum 5-day and 15-day water volumes.

The impacts of climate change on extreme streamflow were also evaluated through the flood frequency analysis of the historical simulations and future projections under the RCP4.5 and RCP8.5 scenarios. The type 3 Pearson distribution (P3), which was used by the U.S. Army Corps of Engineers and recommended by the ministry of water resources of China in flood frequency analysis [76,77], was used for the flood frequency analysis at three mainstream stations of the Yangtze River. The P3 distribution is the generalized gamma distribution and is one of the most commonly used distributions for hydrologic frequency analysis. In an investigation of the fit of theoretical distributions to annual low-flow data, Matalas [78] found the P3 distribution to be one of the most successful models.

3. Results

3.1. Changes in Climate Conditions

Relative to the historical period, the RCM ensemble projects an apparent increase in temperature and no significant increase in precipitation (Figure 3). In the RCP4.5 (RCP8.5) emission scenario, the annual mean temperature is expected to rise on average by 1.81 °C (2.26 °C) and annual precipitation is expected to rise by 3.62% (7.65%) until the middle of this century; however, there was evidence of marked temporal and spatial variability (Table 3). For seasonal changes, temperature, and precipitation are projected to increase and to lead to warmer and wetter conditions for most seasons except autumn (−3.57% under RCP4.5 or −1.97% under RCP8.5). The increases in temperature are more pronounced during colder months in autumn and winter. Figure 4 shows the spatial variability of predicted changes in average annual and seasonal temperature and precipitation in the middle of 21st century (2020–2049) compared to the historical period (1980–2005) under the RCP4.5 and RCP8.5 scenarios. The multi-model ensemble indicates an increase in annual and seasonal temperature in the whole basin. In particular, a larger rise in temperature was found in the lower reach of the Yangtze River basin. Precipitation was projected to decrease over the upstream of the Yangtze River basin and increase over the downstream region.
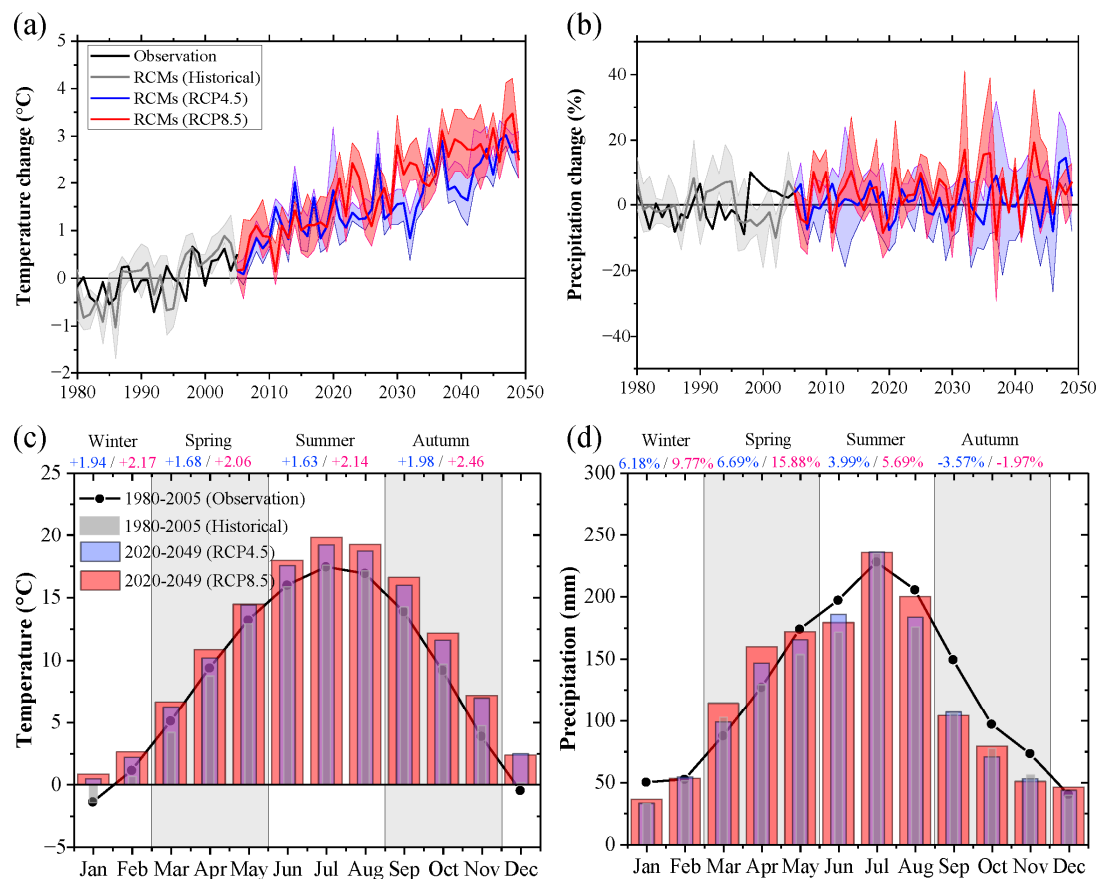
Figure 3. Simulated temperature (**a**) and precipitation (**b**) yearly anomaly (the range of different RCMs is shaded) and seasonal climate patterns in the Yangtze River basin for monthly mean temperature (**c**) and monthly mean precipitation (**d**) for the historical period compared to the mean for future climate conditions.
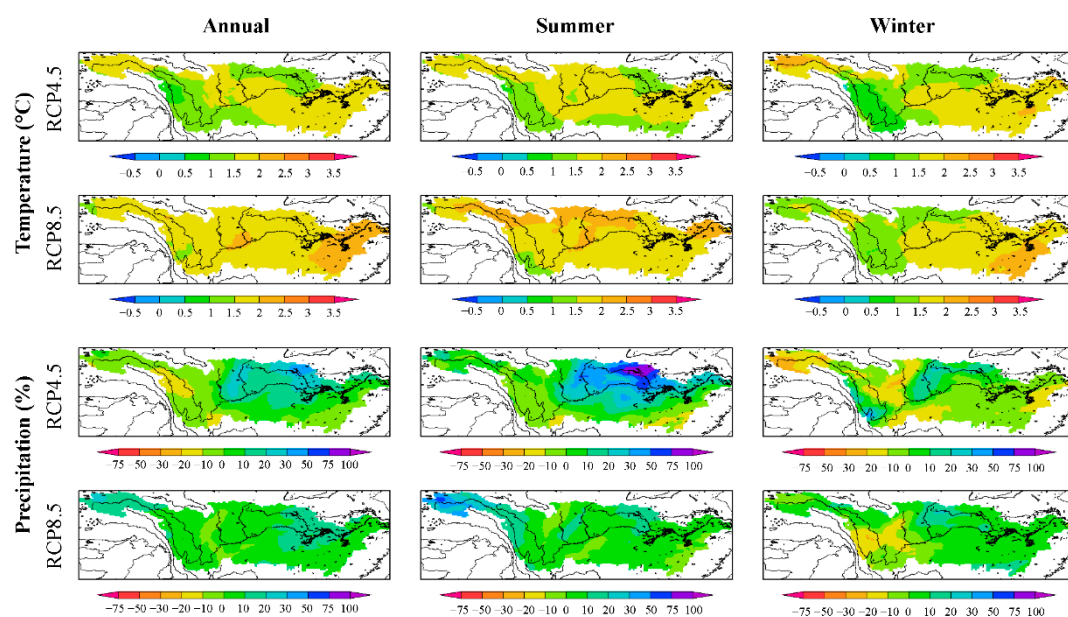

Figure 4. Annual and seasonal changes in mean temperature and precipitation for two emission scenarios (RCP4.5 and RCP8.5) during the mid-century period (2020–2049) relative to the historical period (1980–2005).

The future projections of extreme annual precipitation cumulated over durations of 1, 5, and 10 days in the Yangtze River basin are shown in Figure 5. These nonparametric extreme precipitation indicators are useful for complementing the assessment of future flood hazards. The results show a significantly increasing trend of maximum daily precipitation by the middle of this century. Under the RCP4.5 (RCP8.5) scenario, the future projections indicate a virtually certain increase by 9.13% (10.90%), 9.28% (10.05%), and 9.22% (10.34%) for maximum 1-day, 5-day, and 10-day precipitation, respectively. The increase is only marginally higher under RCP8.5 than under RCP4.5.
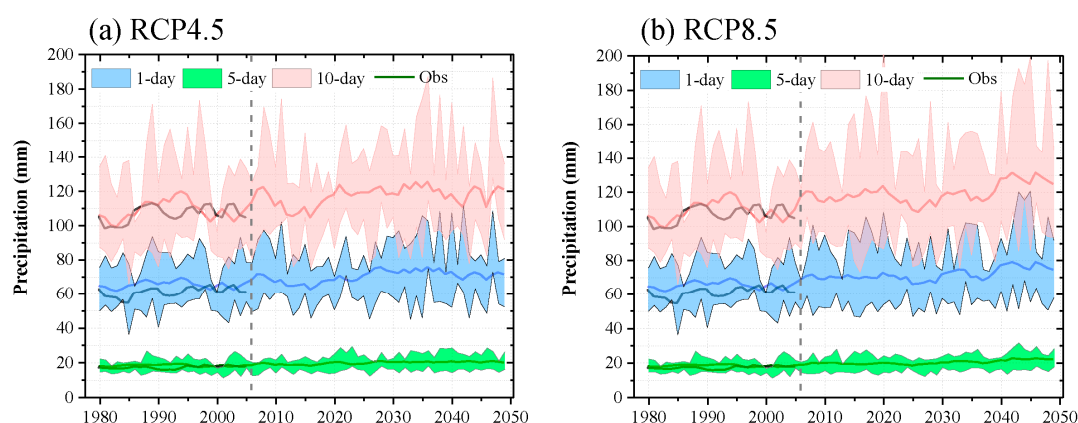

Figure 5. Multi-model ensemble projections of annual maximum precipitation over 1, 5, and 10 days under RCP4.5 (**a**) and RCP8.5 (**b**) scenarios.

3.2. Future Hydrological Extremes

The projection of the monthly averaged streamflow and percentage change in streamflow during the historical period (1980–2005) and during the mid-century period (2020–2049) for two emission scenarios, RCP4.5 and 8.5, are shown in Figure 6. Table 3 shows the future changes in the seasonal temperature, precipitation, evapotranspiration, and streamflow for three watersheds. Due to a projected increase in precipitation and a slight decrease in evapotranspiration, the streamflows of the three mainstream hydrology stations are expected to increase significantly. Overall, a multimodel basin mean increase in streamflow of 11.02% (14.80%) was projected for 2020–2049, with a range between –4.94% and +28.99% (+0.25% and +34.81%) in the RCP4.5 (or RCP8.5) scenario among different models. It is clear that the increase in streamflow was more significant than the increase in precipitation, as was indicated by a non-linear relationship between the two factors. Moreover, it is important to notice the temporal variations in the changes. The streamflow in MAM and JJA were projected to have large increments, which were in agreement with the precipitation increase. The resulting range reflects the large uncertainty associated with the projected future streamflow.

The unexpected result was the slightly decreased trend in the future evapotranspiration projection. In the VIC model, actual evapotranspiration is computed based on a function of potential evapotranspiration calculated using the Penman–Monteith method and the water availability in the soil. Under the future climate scenarios, the RCMs simulated a decrease in the number of rainy days and light rain days, together with an increase in moderate and heavy rain days. For light rain events, runoff response was limited, whereas for heavy rainfall events, a significant increase in runoff was simulated. Take Cuntan as an example, the models projected an increase of 18 mm in annual average precipitation and an increase of 29 mm in annual average runoff in future period under RCP4.5 scenario. Moreover, the historical storm runoff coefficients ranging from 0.49 to 0.54 at different stations were projected to increase by 0.02 to 0.04 in future scenarios, indicating that changes in precipitation are amplified in runoff. These factors may collectively result in declined actual evapotranspiration.

Table 3. Multimodel ensemble average projected seasonal change in temperature, precipitation, evapotranspiration, and streamflow in the future (2020–2049) relative to the historical period (1980–2005) at three mainstream stations in the Yangtze River basin.

| Station	Scenario	Temperature (°C)				Precipitation (%)				Evapotranspiration (%)				Streamflow (%)			
		DJF	MAM	JJA	SON	DJF	MAM	JJA	SON	DJF	MAM	JJA	SON	DJF	MAM	JJA	SON
Cuntan	RCP4.5	1.95	1.95	1.69	2.16	−0.44	2.19	5.12	−5.97	−3.61	−1.65	−1.90	−5.43	−0.69	2.30	6.72	3.07
	RCP8.5	2.23	2.27	2.22	2.68	−0.58	9.19	6.23	−2.62	−2.09	2.27	−2.41	−2.86	1.90	7.64	8.97	4.62
Yichang	RCP4.5	1.89	1.98	1.68	2.02	0.92	3.75	6.09	−5.71	1.35	−1.79	−2.03	−5.37	−0.68	3.34	8.35	3.99
	RCP8.5	2.19	2.31	2.20	2.53	0.77	11.05	6.33	−2.57	1.38	1.21	−2.96	−3.42	1.95	9.32	9.93	5.63
Datong	RCP4.5	1.93	1.79	1.63	1.89	6.41	7.23	7.44	−3.85	5.23	−4.41	−3.98	−8.09	4.72	8.41	13.93	8.90
	RCP8.5	2.17	2.17	2.15	2.37	9.44	16.12	5.81	−2.51	4.50	−3.31	−5.45	−6.89	8.24	17.49	13.45	10.29
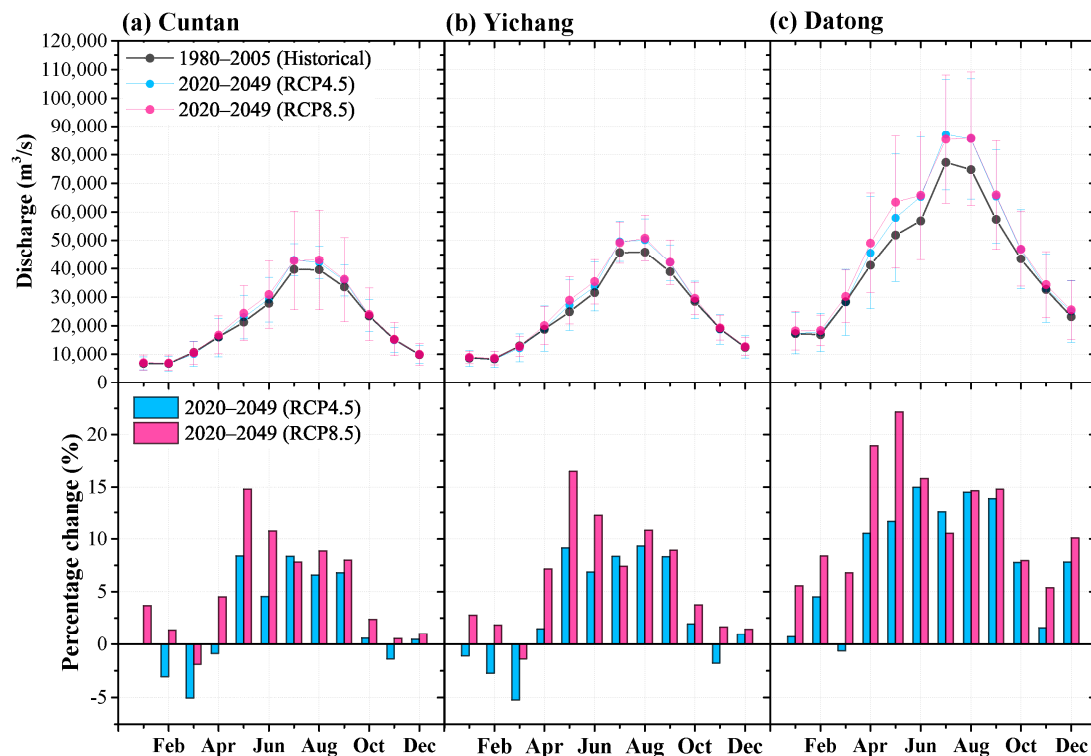
Figure 6. Comparison of monthly averaged streamflow and percentage change in streamflow during the historical period (1980–2005), and during the mid-century period (2020–2049) for two emission scenarios (RCP4.5 and 8.5) at (**a**) Cuntan, (**b**) Yichang, and (**c**) Datong stations. Error bars in the first row show the standard deviation of the multi-model monthly averaged streamflow.

Figure 7 shows the frequency analysis based on the annual extreme maximum streamflow (maximum 1-day streamflow, maximum of 5-day and 15-day water volume) at three mainstream stations. The results indicate that more frequent incidences of flash-flooding at the Cuntan, Yichang, and Datong stations could be expected in the future climate change context, as suggested by the streamflow frequency analysis plots. In addition, Table 4 shows the percentage changes of the extreme streamflow at different return periods (e.g., 2- to 50-year return periods) calculated by the streamflow frequency analysis under the two future climate scenarios compared to the historical period. The ensemble means of extreme maximum streamflow shows an increase in the two future scenarios and the increases are greater in the RCP8.5 scenario for all return periods. Therefore, extreme floods are expected to become more frequent and severe over the Yangtze River basin in the future, especially in the RCP8.5 scenario. In the meantime, evidence such as the increase in maximum 1-day streamflow (+14.24% on average) being larger than the increase in maximum 5-day and 15-day water volumes (+12.79% and +10.24%) implies that this projected extreme streamflow increase would be primarily due to intense short-period rainfall events. The projected increases in the maximum streamflow may greatly increase the risk of flooding and other environmental problems such as soil erosion.
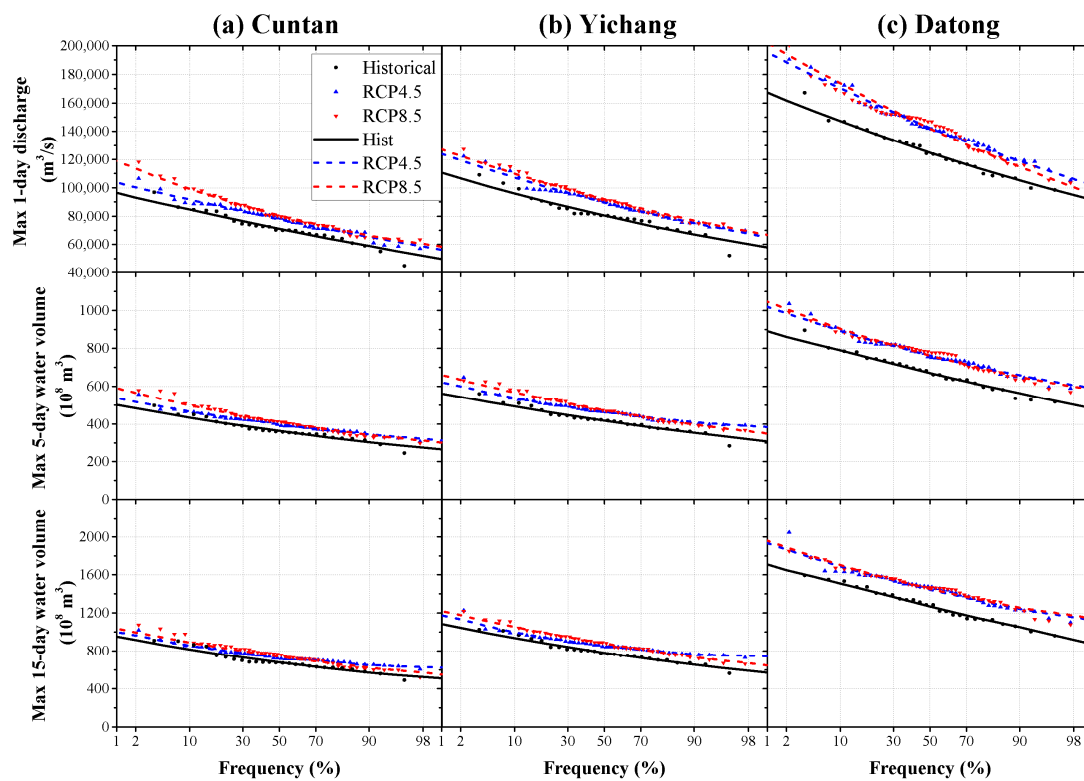
Figure 7. The multi-RCM ensembles (dot) and fitted frequency curve (line) of the annual extreme maximum streamflow (maximum 1-day streamflow, maximum of 5- and 15-day water volumes) for the historical (1980–2005) and changed climate (2020–2049) for (**a**) Cuntan, (**b**) Yichang, and (**c**) Datong stations.

The Mann–Kendall test was used to detect the trend of rainfall and streamflow with Sen's slope estimator (Table 5). A brief description of the tests can be found in Martino et al. [79]. No statistically significant temporal trends at 5% confidence level were identified in historical annual precipitation and streamflow during 1980–2005. The positive trend slopes indicate a slight increase trend in future rainfall and streamflow during 2020–2049, although most of these increases were not statistically significant. Significant increases were found in future extreme streamflows under RCP8.5 scenario, especially in Yichang and Datong stations.

Table 4. Relative percentile change in extreme hydrological indicators for Cuntan, Yichang, and Datong stations during the future period (2020–2049) under RCP4.5 and RCP8.5 scenarios compared with the historical period (1980–2005).

Return Period (Year)	Maximum 1-Day Streamflow (%)						Maximum 5-Day Water Volume (%)						Maximum 15-Day Water Volume (%)					
	Cuntan		Yichang		Datong		Cuntan		Yichang		Datong		Cuntan		Yichang		Datong	
	RCP4.5	RCP8.5	RCP4.5	RCP8.5	RCP4.5	RCP8.5	RCP4.5	RCP8.5	RCP4.5	RCP8.5	RCP4.5	RCP8.5	RCP4.5	RCP8.5	RCP4.5	RCP8.5	RCP4.5	RCP8.5
2	9.64	13.47	11.55	14.38	14.33	13.85	9.76	13.42	10.91	13.76	13.91	13.75	8.30	9.31	9.29	12.59	13.80	14.41
5	8.76	15.42	11.56	14.39	15.26	16.63	8.02	14.38	9.18	14.71	13.04	13.82	5.72	9.30	6.75	12.60	12.04	12.66
10	8.35	17.15	11.67	14.50	15.72	17.95	7.42	15.12	8.99	15.36	13.04	14.41	4.97	9.22	6.50	12.62	11.82	12.58
20	8.04	19.39	11.84	14.68	16.10	18.98	7.21	16.01	9.54	16.08	13.50	15.48	4.88	9.07	7.33	12.67	12.32	13.32
50	7.71	22.27	12.08	14.92	16.52	20.10	7.11	17.12	10.49	16.98	14.24	16.97	5.04	8.87	8.74	12.76	13.20	14.56

Table 5. Trend slopes for precipitation and streamflow at three mainstream stations.

Hydrological Variable	Station	1980–2005	2020–2049	
			RCP4.5	**RCP8.5**
Annual precipitation (mm)	Cuntan	1.55	0.36	**2.91** *
	Yichang	1.28	0.73	2.92
	Datong	1.74	1.46	2.19
Annual average streamflow (m^3/s)	Cuntan	−61	19	22
	Yichang	−59	17	34
	Datong	−13	38	85
Maximum 1-day streamflow (m^3/s)	Cuntan	−211	217	261
	Yichang	−207	254	**294** *
	Datong	430	380	**417** *
Maximum 5-day water volume (10^8 m^3)	Cuntan	−0.68	0.74	0.96
	Yichang	−0.33	0.91	1.06
	Datong	2.74	**1.74** *	**2.20** *
Maximum 15-day water volume (10^8 m^3)	Cuntan	−0.52	0.71	2.49
	Yichang	0.77	1.40	1.75
	Datong	5.2	2.84	**3.49** *

* and bold indicates statistically significant at 5%.

4. Discussion

The Yangtze River basin is very vulnerable to flooding because of the low-lying and broad valley of the lower part of the basin is densely populated. The expenditure on flood protection in Yangtze River basin has grown considerably in recent decades. However, the potential impacts of climate change were not considered in current flood defense system designing and water resources planning in Yangtze River basin. The findings in this study have some implications for policy that the government and non-government agencies should focus on. As a result of the precipitation increment, the projected maximum increment in extreme flood event with 50-year return period is up to 22% over the Yangtze River basin by the middle of this century. The frequency and magnitude of floods are likely to increase in this region. Therefore, a situation in which the design flood level shifts to a higher level than at present should be considered when designing flood control architecture in the study area. The increasing extreme hydrological events suggest the wisdom of re-examining design standard and operating rules of the water conservancy projects for a wider range of climate conditions than traditionally used. The storm runoff coefficients were projected to increase by 0.02 to 0.04 in future scenarios, indicating that the contribution of rainfall to soil moisture will decline. Impacts on soil moisture and evapotranspiration will have important implications on irrigation and agricultural crop and land management.

This study's results should be considered in the context of others studies that used GCM to drive hydrologic models or land surface schemes to project streamflow in the Yangtze River basin [24–30]. Our results are consistent with Su et al. [27], who coupled five bias-corrected CMIP5 GCMs to drive one conceptual hydrologic model and three process-based hydrologic models to produce future streamflow in the upper Yangtze River basin under four RCP scenarios. They found high variability in the simulation results, but 69% of the simulation results derived from 160 combinations of different GCMs, RCPs, and hydrological models projected an increasing trend in the annual average streamflow and 90% of projections showed increasing trends in annual peak streamflow in the 21st century. Bian et al. [30] drove the distributed hydrological soil vegetation model (DHSVM) with statistically downscaled data from six CMIP5 GCMs to project the streamflow dynamics in the source region of the Yangtze River basin under three RCP scenarios. They also projected an increasing trend in seasonal mean streamflow, ranging from −0.52% to 22.58%. However, the findings from this study

are not consistent with some other studies using various single-model approaches. Cao et al. [25] and Zeng et al. [24] projected a decreasing trend in annual streamflow, and especially in summer.

Assessments of future climate change impacts are commonly plagued by uncertainties [80]. Uncertainties can potentially arise from a combination of emission scenarios, GCM structures, downscaling methods, bias corrections, hydrological model structures, and model parameterizations [81]. The GCM structure is the primary source of uncertainty for evaluating hydrological impacts [82,83]. A common approach for curtailing the uncertainty associated with climate models is using an ensemble of different climate models. In this study, we used an ensemble of RCMs for regional hydro-climate projections over the Yangtze River basin, which is helpful in the estimation of future climate-related risks; however, we acknowledge that a number of uncertainties that may have an influence on the simulated hydrological response still exist. For instance, the use of a single GCM underrepresents the uncertainty associated with the GCM's internal variability. Because the simulations of HadGEM2-AO are quite close to the mean of the CMIP5 ensemble [48], it is believed that some parts of the uncertainty from the driving GCMs have been considered in the current simulation. Similarly, the choice of hydrologic model may also influence results at specific locations. Therefore, the results of this study are intended to provide overall and regional trends across the whole Yangtze River basin rather than to get a precise prediction at a specific location.

The results obtained in this study are mainly model/scenario-specific. Moreover, spatio-temporal changes in streamflow will be influenced by comprehensive anthropogenic factors (e.g., reservoir operation, irrigation, land-use change, etc.), which are not considered in the current study. Nevertheless, this study provides a valuable hydrological projection on a local scale as the climate outputs from CORDEX East Asia have the highest spatial resolution up to this point.

5. Conclusions

In this study, we present, to the best of our knowledge, the first examination of projected changes in the Yangtze River basin's streamflow using a suite of RCMs from CORDEX. Our results suggest that between 1980–2005 and 2020–2049, projections of change to the basin's annual mean temperature are expected to rise on average by 1.81 °C (2.26 °C) and annual precipitation by 3.62% (7.65%) under RCP4.5 (or RCP8.5) until the middle of this century. The temperature increase and this small increase in precipitation agree with other analyses of projected changes from CMIP5 models [84–86] and from some RCMs [87–89].

However, we focus on future streamflow changes using climate projections from CORDEX model outputs after bias correction together with a distributed hydrological model. Overall, a multi-model basin average increase in streamflow of 11.02% and 14.80% were projected for 2020–2049 in the RCP4.5 and RCP8.5 scenarios, respectively. It is clear that the increase in streamflow was larger than the increase in precipitation, and the change in streamflow also shows significant temporal and spatial variations and large divergence between regional climate models. At the same time, the maximum streamflow was also projected to increase in the three mainstream stations. In particular, the larger increase in maximum 1-day streamflow (+14.24% on average) compared to the 5-day and 15-day water volumes (+12.79% and +10.24%) indicated that this projected extreme streamflow increase would be primarily due to intense short-period rainfall events. However, these increments were slightly higher than the values that have been reported by our previous study, while an increase of 3.64–10.54% is based on the ensemble mean of 27 CMIP5 GCMs [71]. In addition, the increased trends were identified in future precipitation and streamflow projections, although most of these increases were not statistically significant. To better plan cooperative water resource management, it is necessary to stop just using the climate of the past to plan for the future in the context of climate change.

Conflicts of Interest: The authors declare no conflict of interest.

References

1. Alexander, L.V.; Zhang, X.; Peterson, T.C.; Caesar, J.; Gleason, B.; Klein Tank, A.M.G.; Haylock, M.; Collins, D.; Trewin, B.; Rahimzadeh, F.; et al. Global observed changes in daily climate extremes of temperature and precipitation. *J. Geophys. Res.* **2006**, *111*. [CrossRef]

2. Intergovernmental Panel on Climate Change (IPCC). *Climate Change 2013: The Physical Science Basis. Contribution of Working Group 1 to the Fifth Assessment Report of the Intergovernmental Panel on Climate Change*; Stocker, T.F., Qin, D., Eds.; Cambridge University Press: New York, NY, USA, 2013.

3. Allen, M.R.; Ingram, W.J. Constraints on future changes in climate and the hydrologic cycle. *Nature* **2002**, *419*, 224–232. [CrossRef] [PubMed]

4. Wentz, F.J.; Ricciardulli, L.; Hilburn, K.; Mears, C. How much more rain will global warming bring? *Science* **2007**, *317*, 233–235. [CrossRef] [PubMed]

5. Asadieh, B.; Krakauer, N.Y. Global change in streamflow extremes under climate change over the 21st century. *Hydrol. Earth Syst. Sci.* **2017**, *21*, 5863–5874. [CrossRef]

6. Dankers, R.; Arnell, N.W.; Clark, D.B.; Falloon, P.D.; Fekete, B.A.Z.M.; Gosling, S.N.; Heinke, J.; Kim, H.; Masaki, Y.; Satoh, Y.; et al. First look at changes in flood hazard in the Inter-Sectoral Impact Model Intercomparison Project ensemble. *Proc. Natl. Acad. Sci. USA* **2014**, *111*, 3257–3261. [CrossRef] [PubMed]

7. Trenberth, K.E. Changes in precipitation with climate change. *Clim. Res.* **2011**, *47*, 123–138. [CrossRef]

8. Teutschbein, C.; Grabs, T.; Karlsen, R.H.; Laudon, H.; Bishop, K. Hydrological response to changing climate conditions: Spatial streamflow variability in the boreal region. *Water Resour. Res.* **2015**, *51*, 9425–9446. [CrossRef]

9. Kharel, G.; Kirilenko, A. Comparing CMIP-3 and CMIP-5 climate projections on flooding estimation of Devils Lake of North Dakota, USA. *PeerJ* **2018**, *6*. [CrossRef] [PubMed]

10. Arnell, N.W.; Gosling, S.N. The impacts of climate change on river flood risk at the global scale. *Clim. Chang.* **2016**, *134*, 387–401. [CrossRef]

11. Hirabayashi, Y.; Mahendran, R.; Koirala, S.; Konoshima, L.; Yamazaki, D.; Watanabe, S.; Kim, H.; Kanae, S. Global flood risk under climate change. *Nat. Clim. Chang.* **2013**, *3*, 816–821. [CrossRef]

12. Kharel, G.; Zheng, H.; Kirilenko, A. Can land-use change mitigate long-term flood risks in the Prairie Pothole Region? The case of Devils Lake, North Dakota, USA. *Reg. Environ. Chang.* **2016**, *16*, 2443–2456. [CrossRef]

13. Wang, X.; Yang, T.; Li, X.; Shi, P.; Zhou, X. Spatio-temporal changes of precipitation and temperature over the Pearl River basin based on CMIP5 multi-model ensemble. *Stoch. Environ. Res. Risk Assess.* **2017**, *31*, 1077–1089. [CrossRef]

14. Wang, X.; Yang, T.; Yong, B.; Krysanova, V.; Shi, P.; Li, Z.; Zhou, X. Impacts of climate change on flow regime and sequential threats to riverine ecosystem in the source region of the Yellow River. *Environ. Earth Sci.* **2018**, *77*, 465. [CrossRef]

15. Jiang, Z.; Song, J.; Li, L.; Chen, W.; Wang, Z.; Wang, J. Extreme climate events in China: IPCC-AR4 model evaluation and projection. *Clim. Chang.* **2012**, *110*, 385–401. [CrossRef]

16. Chen, H. Projected change in extreme rainfall events in China by the end of the 21st century using CMIP5 models. *Chin. Sci. Bull.* **2013**, *58*, 1462–1472. [CrossRef]

17. Yira, Y.; Diekkruger, B.; Steup, G.; Bossa, A.Y. Impact of climate change on hydrological conditions in a tropical West African catchment using an ensemble of climate simulations. *Hydrol. Earth Syst. Sci.* **2017**, *21*, 2143–2161. [CrossRef]

18. Seneviratne, S.I.; Rogelj, J.; Séférian, R.; Wartenburger, R.; Allen, M.R.; Cain, M.; Millar, R.J.; Ebi, K.L.; Ellis, N.; Hoegh-Guldberg, O.; et al. The many possible climates from the Paris Agreement's aim of 1.5 °C warming. *Nature* **2018**, *558*, 41–49. [CrossRef] [PubMed]

19. Guan, Y.; Zheng, F.; Zhang, X.; Wang, B. Trends and variability of daily precipitation and extremes during 1960–2012 in the Yangtze River Basin, China. *Int. J. Climatol.* **2017**, *37*, 1282–1298. [CrossRef]

20. Su, B.D.; Jiang, T.; Jin, W.B. Recent trends in observed temperature and precipitation extremes in the Yangtze River basin, China. *Theor. Appl. Climatol.* **2006**, *83*, 139–151. [CrossRef]

21. Birkinshaw, S.J.; Guerreiro, S.B.; Nicholson, A.; Liang, Q.; Quinn, P.; Zhang, L.; He, B.; Yin, J.; Fowler, H.J. Climate change impacts on Yangtze River discharge at the Three Gorges Dam. *Hydrol. Earth Syst. Sci.* **2017**, *21*, 1911–1927. [CrossRef]

22. Xie, P.; Wu, J.; Huang, J.; Han, X. Three-Gorges Dam: Risk to ancient fish. *Science* **2003**, *302*, 1149–1151. [CrossRef] [PubMed]

23. Yin, H.; Li, C. Human impact on floods and flood disasters on the Yangtze River. *Geomorphology* **2001**, *41*, 105–109. [CrossRef]

24. Zeng, X.; Kundzewicz, Z.W.; Zhou, J.; Su, B. Discharge projection in the Yangtze River basin under different emission scenarios based on the artificial neural networks. *Quat. Int.* **2012**, *282*, 113–121. [CrossRef]

25. Cao, L.; Zhang, Y.; Shi, Y. Climate change effect on hydrological processes over the Yangtze River basin. *Quat. Int.* **2011**, *244*, 202–210. [CrossRef]

26. Chen, H.; Xiang, T.; Zhou, X.; Xu, C. Impacts of climate change on the Qingjiang Watershed's runoff change trend in China. *Stoch. Environ. Res. Risk Assess.* **2012**, *26*, 847–858. [CrossRef]

27. Su, B.; Huang, J.; Zeng, X.; Gao, C.; Jiang, T. Impacts of climate change on streamflow in the Upper Yangtze River basin. *Clim. Chang.* **2017**, *141*, 533–546. [CrossRef]

28. Woo, M.; Long, T.; Thorne, R. Simulating monthly streamflow for the Upper Changjiang, China, under climatic change scenarios. *Hydrol. Sci. J.* **2009**, *54*, 596–605. [CrossRef]

29. Xu, H.; Taylor, R.G.; Xu, Y. Quantifying uncertainty in the impacts of climate change on river discharge in sub-catchments of the Yangtze and Yellow River Basins, China. *Hydrol. Earth Syst. Sci.* **2011**, *15*, 333–344. [CrossRef]

30. Bian, H.; Lü, H.; Sadeghi, A.M.; Zhu, Y.; Yu, Z.; Ouyang, F.; Su, J.; Chen, R. Assessment on the effect of climate change on streamflow in the source region of the Yangtze River, China. *Water* **2017**, *9*. [CrossRef]

31. Feng, Y.; Zhou, J.; Mo, L.; Yuan, Z.; Zhang, P.; Wu, J.; Wang, C.; Wang, Y. Long-term hydropower generation of cascade reservoirs under future climate changes in Jinsha River in Southwest China. *Water* **2018**, *10*. [CrossRef]

32. Wang, X.; Yang, T.; Wortmann, M.; Shi, P.; Hattermann, F.; Lobanova, A.; Aich, V. Analysis of multi-dimensional hydrological alterations under climate change for four major river basins in different climate zones. *Clim. Chang.* **2017**, *141*, 483–498. [CrossRef]

33. Gu, H.; Wang, G.; Yu, Z.; Mei, R. Assessing future climate changes and extreme indicators in east and south Asia using the RegCM4 regional climate model. *Clim. Chang.* **2012**, *114*, 301–317. [CrossRef]

34. Giménez, P.; García-Galiano, S. Assessing regional climate models (RCMs) ensemble-driven reference evapotranspiration over Spain. *Water* **2018**, *10*. [CrossRef]

35. Park, C.; Min, S.; Lee, D.; Cha, D.; Suh, M.; Kang, H.; Hong, S.; Lee, D.; Baek, H.; Boo, K.; et al. Evaluation of multiple regional climate models for summer climate extremes over East Asia. *Clim. Dyn.* **2016**, *46*, 2469–2486. [CrossRef]

36. Huang, B.; Polanski, S.; Cubasch, U. Assessment of precipitation climatology in an ensemble of CORDEX-East Asia regional climate simulations. *Clim. Res.* **2015**, *64*, 141–158. [CrossRef]

37. Gu, H.; Yu, Z.; Yang, C.; Ju, Q.; Yang, T.; Zhang, D. High-resolution ensemble projections and uncertainty assessment of regional climate change over China in CORDEX East Asia. *Hydrol. Earth Syst. Sci.* **2018**, *22*, 3087–3103. [CrossRef]

38. Moss, R.H.; Edmonds, J.A.; Hibbard, K.A.; Manning, M.R.; Rose, S.K.; van Vuuren, D.P.; Carter, T.R.; Emori, S.; Kainuma, M.; Kram, T.; et al. The next generation of scenarios for climate change research and assessment. *Nature* **2010**, *463*, 747–756. [CrossRef] [PubMed]

39. Liu, J.P.; Xu, K.H.; Li, A.C.; Milliman, J.D.; Velozzi, D.M.; Xiao, S.B.; Yang, Z.S. Flux and fate of Yangtze River sediment delivered to the East China Sea. *Geomorphology* **2007**, *85*, 208–224. [CrossRef]

40. Wang, H.; Saito, Y.; Zhang, Y.; Bi, N.; Sun, X.; Yang, Z. Recent changes of sediment flux to the western Pacific Ocean from major rivers in East and Southeast Asia. *Earth-Sci. Rev.* **2011**, *108*, 80–100. [CrossRef]

41. Lu, X.X. Vulnerability of water discharge of large Chinese rivers to environmental changes: An overview. *Reg. Environ. Chang.* **2004**, *4*, 182–191. [CrossRef]

42. Yang, S.L.; Liu, Z.; Dai, S.B.; Gao, Z.X.; Zhang, J.; Wang, H.J.; Luo, X.X.; Wu, C.S.; Zhang, Z. Temporal variations in water resources in the Yangtze River (Changjiang) over the Industrial Period based on reconstruction of missing monthly discharges. *Water Resour. Res.* **2010**, *46*. [CrossRef]

43. Verdin, K.L.; Verdin, J.P. A topological system for delineation and codification of the Earth's river basins. *J. Hydrol.* **1999**, *218*, 1–12. [CrossRef]

44. Food and Agriculture Organization (FAO). Digital soil map of the world and derived soil properties. In *Land Water Digital Media Series*; FAO: Rome, Italy, 1997.

45. Hansen, M.C.; Defries, R.S.; Yownshend, J.R.G.; Sohlberg, R. Global land cover classification at 1 km spatial resolution using a classification tree approach. *Int. J. Remote Sens.* **2000**, *21*, 1331–1364. [CrossRef]

46. Li, Q.; Wang, S.; Lee, D.; Tang, J.; Niu, X.; Hui, P.; Gutowski, W.J.; Dairaku, K.; McGregor, J.L.; Katzfey, J.; et al. Building Asian climate change scenario by multi-regional climate models ensemble. Part II: Mean precipitation. *Int. J. Climatol.* **2016**, *36*, 4253–4264. [CrossRef]

47. Suh, M.S.; Oh, S.G.; Lee, D.K.; Cha, D.H.; Choi, S.J.; Jin, C.S.; Hong, S.Y. Development of new ensemble methods based on the performance skills of regional climate models over South Korea. *J. Clim.* **2012**, *25*, 7067–7082. [CrossRef]

48. Gu, H.; Yu, Z.; Wang, J.; Wang, G.; Yang, T.; Ju, Q.; Yang, C.; Xu, F.; Fan, C. Assessing CMIP5 general circulation model simulations of precipitation and temperature over China. *Int. J. Climatol.* **2015**, *35*, 2431–2440. [CrossRef]

49. Davies, T.; Cullen, M.J.P.; Malcolm, A.J.; Mawson, M.H.; Staniforth, A.; White, A.A.; Wood, N. A new dynamical core for the Met Office's global and regional modelling of the atmosphere. *Q. J. R. Meteorol. Soc.* **2005**, *131*, 1759–1782. [CrossRef]

50. Skamarock, W.C.; Klemp, J.B.; Dudhia, J.; Gill, D.O.; Barker, D.M.; Wang, W.; Powers, J.G. *A Description of the Advanced Research WRF Version 2*; National Center for Atmospheric Research: Boulder, CO, USA, 2005.

51. Cha, D.; Lee, D. Reduction of systematic errors in regional climate simulations of the summer monsoon over East Asia and the western North Pacific by applying the spectral nudging technique. *J. Geophys. Res. Atmos.* **2009**, *114*. [CrossRef]

52. Giorgi, F.; Coppola, E.; Solmon, F.; Mariotti, L.; Sylla, M.B.; Bi, X.; Elguindi, N.; Diro, G.T.; Nair, V.; Giuliani, G.; et al. RegCM4: Model description and preliminary tests over multiple CORDEX domains. *Clim. Res.* **2012**, *52*, 7–29. [CrossRef]

53. Hong, S.; Park, H.; Cheong, H.; Kim, J.E.; Koo, M.; Jang, J.; Ham, S.; Hwang, S.; Park, B.; Chang, E.; et al. The global/regional integrated model system (GRIMs). *Asia-Pac. J. Atmos. Sci.* **2013**, *49*, 219–243. [CrossRef]

54. Maraun, D.; Shepherd, T.G.; Widmann, M.; Zappa, G.; Walton, D.; Gutiérrez, J.M.; Hagemann, S.; Richter, I.; Soares, P.M.M.; Hall, A.; et al. Towards process-informed bias correction of climate change simulations. *Nat. Clim. Chang.* **2017**, *7*, 764–773. [CrossRef]

55. Teutschbein, C.; Seibert, J. Bias correction of regional climate model simulations for hydrological climate-change impact studies: Review and evaluation of different methods. *J. Hydrol.* **2012**, *456–457*, 12–29. [CrossRef]

56. Gu, H.; Yu, Z.; Wang, G.; Wang, J.; Ju, Q.; Yang, C.; Fan, C. Impact of climate change on hydrological extremes in the Yangtze River Basin, China. *Stoch. Environ. Res. Risk Assess.* **2015**, *29*, 693–707. [CrossRef]

57. Piani, C.; Haerter, J.O.; Coppola, E. Statistical bias correction for daily precipitation in regional climate model over Europe. *Theor. Appl. Climatol.* **2010**, *99*, 187–192. [CrossRef]

58. Block, P.J.; Souza Filho, F.A.; Sun, L.; Kwon, H.H. A streamflow forecasting framework using multiple climate and hydrological models. *J. Am Water Resour. Assoc.* **2009**, *45*, 828–843. [CrossRef]

59. Thrasher, B.; Maurer, E.P.; McKellar, C.; Duffy, P.B. Technical Note: Bias correcting climate model simulated daily temperature extremes with quantile mapping. *Hydrol. Earth Syst. Sci.* **2012**, *16*, 3309–3314. [CrossRef]

60. Wood, E.F.; Lettenmaier, D.P.; Zartarian, V.G. A land-surface hydrology parameterization with subgrid variability for general circulation models. *J. Geophys. Res. Atmos.* **1992**, *97*, 2717–2728. [CrossRef]

61. Hidalgo, H.G.; Amador, J.A.; Alfaro, E.J.; Quesada, B. Hydrological climate change projections for Central America. *J. Hydrol.* **2013**, *495*, 94–112. [CrossRef]

62. Nijssen, B.; Schnur, R.; Lettenmaier, D.P. Global retrospective estimation of soil moisture using the variable infiltration capacity land surface model, 1980–93. *J. Clim.* **2001**, *14*, 1790–1808. [CrossRef]

63. Xue, X.; Zhang, K.; Hong, Y.; Gourley, J.J.; Kellogg, W.; McPherson, R.A.; Wan, Z.; Austin, B.N. New multisite cascading calibration approach for hydrological models: Case study in the red river basin using the VIC model. *J. Hydrol. Eng.* **2016**, *21*. [CrossRef]

64. Zhou, S.Q.; Liang, X.; Chen, J.; Gong, P. An assessment of the VIC-3L hydrological model for the Yangtze River basin based on remote sensing: A case study of the Baohe River basin. *Can. J. Remote Sens.* **2004**, *30*, 840–853. [CrossRef]

65. Guo, S.; Guo, J.; Zhang, J.; Chen, H. VIC distributed hydrological model to predict climate change impact in the Hanjiang basin. *Sci. China Ser. E Technol. Sci.* **2009**, *52*, 3234–3239. [CrossRef]

66. Liang, X.; Lettennmaier, D.P.; Wood, E.F.; Burges, S.J. A simple hydrologically based model of land surface water and energy fluxes for general circulation models. *J. Geophys. Res. Atmos.* **1994**, *99*, 14415–14428. [CrossRef]

67. Sheffield, J.; Goteti, G.; Wen, F.; Wood, E.F. A simulated soil moisture based drought analysis for the United States. *J. Geophys. Res. Atmos.* **2004**, *109*. [CrossRef]

68. Liang, X.; Wood, E.F.; Lettennmaier, D.P. Surface soil moisture parameterization of the VIC-2L model: Evaluation and modifications. *Glob. Planet. Chang.* **1996**, *13*, 195–206. [CrossRef]

69. Li, H.; Wigmosta, M.S.; Wu, H.; Huang, M.; Ke, Y.; Coleman, A.M.; Leung, L.R. A physically based runoff routing model for land surface and earth system models. *J. Hydrometeorol.* **2013**, *14*, 808–828. [CrossRef]

70. Yang, Z.; Wang, H.; Saito, Y.; Milliman, J.D.; Xu, K.; Qiao, S.; Shi, G. Dam impacts on the Changjiang (Yangtze) River sediment discharge to the sea: The past 55 years and after the Three Gorges Dam. *Water Resour. Res.* **2006**, *42*. [CrossRef]

71. Yu, Z.; Gu, H.; Wang, J.; Xia, J.; Lu, B. Effect of projected climate change on the hydrological regime of the Yangtze River Basin, China. *Stoch. Environ. Res. Risk Assess.* **2018**, *32*, 1–16. [CrossRef]

72. Duan, Q.Y.; Gupta, V.K.; Sorooshian, S. Shuffled complex evolution approach for effective and efficient global minimization. *J. Optim. Theory Appl.* **1993**, *76*, 501–521. [CrossRef]

73. Nash, J.E.; Sutcliffe, J.V. River flow forecasting through conceptual models 1: A discussion of priciples. *J. Hydrol.* **1970**, *10*, 282–290. [CrossRef]

74. Moriasi, D.N.; Gitau, M.W.; Pai, N.; Daggupati, P. Hydrologic and water quality models: Performance measures and evaluation criteria. *Trans. ASABE* **2015**, *58*, 1763–1785.

75. Gaál, L.; Szolgay, J.; Kohnová, S.; Hlavčová, K.; Parajka, J.; Viglione, A.; Merz, R.; Blöschl, G. Dependence between flood peaks and volumes: A case study on climate and hydrological controls. *Hydrol. Sci. J.* **2015**, *60*, 968–984. [CrossRef]

76. The Ministry of Water Resources of the People's Republic of China. *Regulation for Calculating Design Flood of Water Resources and Hydropower Projects (LS44-93)*; China Water Power Press: Beijing, China, 1993. (In Chinese)

77. Koutrouvelis, I.A.; Canavos, G.C. Estimation in the Pearson type 3 distribution. *Water Resour. Res.* **1999**, *35*, 2693–2704. [CrossRef]

78. Matalas, N.C. *Probability Distribution of Low Flows*; 434A; U.S. Geological Survey: Reston, VA, USA, 1963.

79. Martino, G.D.; Fontana, N.; Marini, G.; Singh, V.P. Variability and trend in seasonal precipitation in the continental United States. *J. Hydrol. Eng.* **2013**, *18*, 630–640. [CrossRef]

80. Knutti, R.; Sedláček, J. Robustness and uncertainties in the new CMIP5 climate model projections. *Nat. Clim. Chang.* **2012**, *3*, 369–373. [CrossRef]

81. Wilby, R.L.; Harris, I. A framework for assessing uncertainties in climate change impacts: Low-flow scenarios for the River Thames, UK. *Water Resour. Res.* **2006**, *42*. [CrossRef]

82. Steinschneider, S.; Wi, S.; Brown, C. The integrated effects of climate and hydrologic uncertainty on future flood risk assessments. *Hydrol. Process.* **2015**, *29*, 2823–2839. [CrossRef]

83. Bennett, K.E.; Werner, A.T.; Schnorbus, M. Uncertainties in hydrologic and climate change impact analyses in headwater basins of British Columbia. *J. Clim.* **2012**, *25*, 5711–5730. [CrossRef]

84. Pan, Z.; Zhang, Y.; Liu, X.; Gao, Z. Current and future precipitation extremes over Mississippi and Yangtze River basins as simulated in CMIP5 models. *J. Earth Sci.* **2016**, *27*, 22–36. [CrossRef]

85. Moriasi, D.N.; Arnold, J.G.; Van Liew, M.W.; Bingner, R.L.; Harmel, R.D.; Veith, T.L. Model evaluation guidelines for systematic quantification of accuracy in watershed simulations. *Trans. ASABE* **2007**, *50*, 885–900. [CrossRef]

86. Sun, Q.; Miao, C.; Duan, Q. Projected changes in temperature and precipitation in ten river basins over China in 21st century. *Int. J. Climatol.* **2015**, *35*, 1125–1141. [CrossRef]

87. Oh, S.; Park, J.; Lee, S.; Suh, M. Assessment of the RegCM4 over East Asia and future precipitation change adapted to the RCP scenarios. *J. Geophys. Res. Atmos.* **2014**, *119*, 2913–2927. [CrossRef]

88. Qin, P.; Xie, Z. Detecting changes in future precipitation extremes over eight river basins in China using RegCM4 downscaling. *J. Geophys. Res. Atmos.* **2016**, *121*, 6802–6821. [CrossRef]

89. Zhu, J.; Huang, G.; Wang, X.; Cheng, G.; Wu, Y. High-resolution projections of mean and extreme precipitations over China through PRECIS under RCPs. *Clim. Dyn.* **2018**, *50*, 4037–4060. [CrossRef]